DOI: 10.1021/ic101273y

Inorganic Chemistry
Article

Tri- and Tetranuclear Nickel(II) Inverse Metallacrown Complexes Involving Oximato Oxygen Linkers: Role of the Guest Anion (Oxo versus Alkoxo) in Controlling the Size of the Ring Topology

Anandalok Audhya,[†] Manoranjan Maity,[†] Kisholoy Bhattacharya,[†] Rodolphe Clérac,[‡,§] and Muktimoy Chaudhury*[,†]

[†]*Department of Inorganic Chemistry, Indian Association for the Cultivation of Science, Kolkata 700 032, India,* [‡]*CNRS, UPR 8641, Centre de Recherche Paul Pascal (CRPP), Equipe "Matériaux Moléculaires Magnétiques", 115 avenue du Dr. Albert Schweitzer, Pessac F-33600, France, and* [§]*Université de Bordeaux, UPR 8641, Pessac F-33600, France*

Received June 26, 2010

A trinuclear oximato complex, $[(NiHL^1)_3(\mu_3\text{-}O)]ClO_4$ (**1**), with inverse metallacrown 9-MC-3 topology has been synthesized using a Schiff-base ligand (H_2L^1) formed by condensation of ethanolamine (Hea) and diacetylmonoxime (Hdamo). The diamagnetic compound has been characterized by electrospray ionization mass spectrometry as well as by single-crystal X-ray diffraction analysis. In the solid state, the alcoholic OH group in this molecule stays away from coordination. Surprisingly in a similar chemical reaction, when intact Hea and Hdamo have been used as ligands instead of their Schiff-base forms, the product obtained is a 12-MC-4-type metallacrown, $(Et_3NH)[Ni_4(damo)_4(Hea)_2(ea)_2](ClO_4)_3$ (**2**), with a larger cavity size needed to accommodate a pair of hydrogen-bonded $(O-H\cdots O)^-$ anions. Unlike in **1**, the alcoholic OH groups in **2** take part in metal coordination. Compound **2** on being refluxed with lithium hydroxide in methanol is converted to **1** in almost quantitative yield. This appears to be a novel reaction type, leading to contraction of a metallacrown ring size. A family of 12-MC-4 Ni_4 metallacrowns in inverse topology, viz., $[Ni_4(damo)_4(H_2dea)_2(Hdea)_2](ClO_4)_2\cdot 2H_2O$ (**3**), $[Ni_4(dpko)_4(Hea)_2(ea)_2](ClO_4)_2\cdot 4H_2O$ (**4**), and $[Ni_4(mpko)_4(Hmea)_2(mea)_2](ClO_4)_2$ (**5**), have been synthesized following a methodology similar to that adopted for **2**, using different combinations of free oximes [viz., dipyridylketonoxime (Hdpko) and methylpyridylketonoxime (Hmpko)] and amino alcohols [viz., diethanolamine (H_2dea), and *N*-methylethanolamine (Hmea)]. Crystal and molecular structures of **3**–**5** have been reported, each involving either a quasi (in **3**) or a perfect (in **4** and **5**) square plane (S_4 symmetry) with four octahedral Ni centers occupying the corners, and serve as a backbone of puckered metallacrown rings that accommodate a pair of hydrogen-bonded $(O-H\cdots O)^-$ anions. Antiferromagnetic interactions within the $[Ni_4]$ core [$J/k_B \approx -20$ to -27 K based on the following spin Hamiltonian: $H=-2J(S_1\cdot S_2 + S_2\cdot S_3 + S_3\cdot S_4 + S_4\cdot S_1)$] lead to an $S_T=0$ ground state for these complexes.

Introduction

Metallacrowns are a type of metallacycle that can be considered as inorganic analogues of crown ethers because of the similarities they have both in structure and in function.[1] These compounds usually have a combination of a transition-metal ion and a heteroatom (usually nitrogen)

*To whom correspondence should be addressed. E-mail: icmc@iacs.res.in.

(1) (a) Pecoraro, V. L.; Stemmler, A. J.; Gibney, B. R.; Bodwin, J. J.; Wang, H.; Kampf, J. N.; Barwinski, A. *Prog. Inorg. Chem.* **1997**, *45*, 83. (b) Bodwin, J. J.; Cutland, A. D.; Malkani, R. G.; Pecoraro, V. L. *Coord. Chem. Rev.* **2001**, *216–217*, 489. (c) Mezei, G.; Zaleski, C. M.; Pecoraro, V. L. *Chem. Rev.* **2007**, *107*, 4933.

(2) For example, see: (a) Stemmler, A. J.; Kampf, J. W.; Kirk, M. L.; Atasi, B. H.; Pecoraro, V. L. *Inorg. Chem.* **1999**, *38*, 2807. (b) Stemmler, A. J.; Barwinski, A.; Bodwin, J. J.; Young, V.; Pecoraro, V. L. *J. Am. Chem. Soc.* **1996**, *118*, 11962. (c) Johnson, J. A.; Kampf, J. W.; Pecoraro, V. L. *Angew. Chem., Int. Ed.* **2003**, *42*, 546. (d) Tegoni, M.; Dallavalle, F.; Belosi, B.; Remelli, M. *Dalton Trans.* **2004**, 1329. (e) Cutland, A. D.; Halfen, J. A.; Kampf, J. W.; Pecoraro, V. L. *J. Am. Chem. Soc.* **2001**, *123*, 6211. (f) Tegoni, M.; Remelli, M.; Bacco, D.; Marchió, L.; Dallavalle, F. *Dalton Trans.* **2008**, 2693. (g) Mezei, G.; Kampf, J. W.; Pan, S.; Poeppelmeier, K. R.; Watkins, B.; Pecoraro, V. L. *Chem. Commun.* **2007**, 1148. (h) Tegoni, M.; Tropiano, M.; Marchió, L. *Dalton Trans.* **2009**, 6705. (i) Lim, C.-S.; Kampf, J. W.; Pecoraro, V. L. *Inorg. Chem.* **2009**, *48*, 5224. (j) Dallavalle, F.; Remelli, M.; Sansone, F.; Bacco, D.; Tegoni, M. *Inorg. Chem.* **2010**, *49*, 1761. (k) Tegoni, M.; Furlotti, M.; Tropiano, M.; Lim, C. S.; Pecoraro, V. L. *Inorg. Chem.* **2010**, *49*, 5190. (l) Zaleski, C. M.; Cutland-Van Noord, A. D.; Kampf, J. W.; Pecoraro, V. L. *Cryst. Growth Des.* **2007**, *7*, 1098. (m) Tegoni, M.; Ferretti, L.; Sansone, F.; Remelli, M.; Bertolasi, V.; Dallavalle, F. *Chem.—Eur. J.* **2007**, *13*, 1300.

(3) For example, see: (a) Butter, R. J.; O'connor, C. J.; Sinn, E. *Inorg. Chem.* **1981**, *20*, 537. (b) Stamatatos, T. C.; Dionyssopoulou, S.; Efthymiou, G.; Kyritsis, P.; Raptopoulou, C. P.; Terzis, A.; Vicente, R.; Escuer, A.; Perlepes, S. P. *Inorg. Chem.* **2005**, *44*, 3374. (c) Afrati, T.; Pantazaki, A. A.; Dendrinou-Samara, C.; Raptopoulou, C.; Terzis, A.; Kessissoglou, D. P. *Dalton Trans.* **2010**, *39*, 765. (d) Dendrinou-Samara, C.; Zaleski, C. M.; Evagorou, A.; Kampf, J. W.; Pecoraro, V. L.; Kessissoglou, D. P. *Chem. Commun.* **2003**, 2668. (e) Stamatatos, T. C.; Foguet-Albiol, D.; Stoumpos, C. C.; Raptopoulou, C. P.; Terzis, A.; Wernsdorfer, W.; Perlepes, S. P.; Chrisotu, G. *J. Am. Chem. Soc.* **2005**, *127*, 15380. (f) Zaleski, C. M.; Wang, T.-C.; Dendrinou-Samara, C.; Alexiou, M.; Kanakavaki, P.; Hsieh, W. Y.; Kampf, J. W.; Penner-Hahn, J. E.; Pecoraro, V. L.; Kessissoglou, D. P. *Inorg. Chem.* **2008**, *47*, 6127. (g) Afrati, T.; Dendrinou-Samara, C.; Raptopoulou, C. P.; Terzis, A.; Tangoulis, V.; Kessissoglou, D. P. *Angew. Chem., Int. Ed.* **2002**, *41*, 2148. (h) Jones, L. F.; Prescimone, A.; Evangelisti, M.; Brechin, E. K. *Chem. Commun.* **2009**, 2023. (i) Milios, C. J.; Inglis, R.; Vinslava, A.; Bagai, R.; Wernsdorfer, W.; Parasons, S.; Perlepes, S. P.; Christou, G.; Brechin, E. K. *J. Am. Chem. Soc.* **2007**, *129*, 12505. (j) Milios, C. J.; Raptopoulou, C. P.; Terzis, A.; Lloret, F.; Vicente, R.; Perlepes, S. P.; Escuer, A. *Angew. Chem., Int. Ed.* **2004**, *43*, 210. (k) Xu, H.-B.; Wang, B.-W.; Pan, F.; Wang, Z.-M.; Gao, S. *Angew. Chem., Int. Ed.* **2007**, *46*, 7388. (l) Stamatatos, T. C.; Luis, B. S.; Moulton, B.; Christou, G. *Inorg. Chem.* **2008**, *47*, 1134.

Published on Web 08/27/2010

that serves as a replacement for the repeating methylene C atoms in the parent crown ether. Hydroxamic acids[2] and oximes[3] have been used traditionally as ligands either exclusively or in tandem[4] for the synthesis of metallacrowns. Various other organic molecules[5] have also been used as linkers to synthesize diverse types of metallacycles that include metallacoronates,[6] azametallacrowns,[7] and metallawheels,[8] which show a closer resemblance with metallacrowns in their structures. Interesting aspects of these molecular assemblies are the presence of multiple metal centers in close proximity that give rise to many interesting properties that include molecular recognition,[9] ion sensing,[10] single-molecule-magnet properties,[11] catalysis,[12] etc.

As a sequel to our long-standing interest in the coordination chemistry of group 10 metal ions (mainly Ni^{II} and Pd^{II}),[13] we have reported recently a family of 9-MC-3-type inverse metallacrown complexes $[(M^{II}L)_3(\mu_3\text{-}O)]ClO_4$ (M = Ni, Pd) involving a discrete $[M^{II}{}_3(\mu_3\text{-}O)]$ core, with HL being a member of a series of tridentate Schiff-base ligands based on diacetylmonoxime (Hdamo).[14] The μ_3-O^{2-} anion in these molecules is reluctant to undergo protonation, unlike many copper(II) complexes of similar topology.[15] In this follow-up work, we have decided to use oximes and amino alcohols together as the ligand, both of which individually are capable of generating metallacycles of different kinds.[3,16] Our motivation this time is to force the inclusion of OH donors of alcohol into the metallacrown cavity and see how this influences the overall topology of the ring. For this, we have chosen Hdamo, di-2-pyridylketonoxime (Hdpko), and methyl-2-pyridylketonoxime (Hmpko) as the coordinating oximes and ethanolamine (Hea), diethanolamine (H_2dea), and *N*-methylethanolamine (Hmea) as the bridging amino alcohols, all shown in Chart 1. Herein, we report the syntheses of both 9-MC-3- and 12-MC-4-type inverse metallacrown complexes of nickel(II) under different reaction conditions as well as their conversion from one to the other in a particular case. Detailed characterizations of these compounds by single-crystal X-ray diffraction analysis as well as by ^{1}H NMR and electrospray ionization mass spectroscopy (ESI-MS) are described. In addition, the magnetic properties of tetranuclear complexes have also been studied.

Chart 1. Oximes and Amino Alcohols Used in the Syntheses of Compounds **1**−**5**

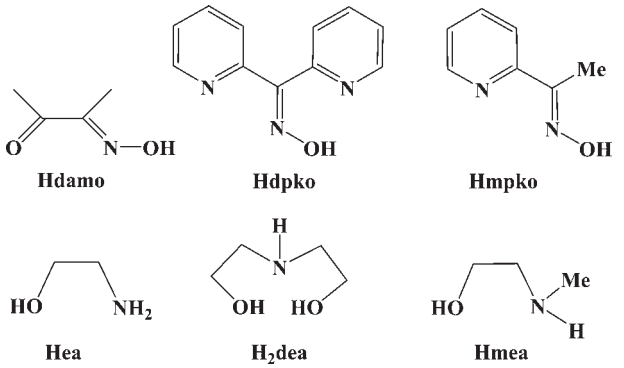

Experimental Section

Materials. All reactions were carried out in an aerobic environment with chemicals available from commercial sources and used as received. Solvents were reagent-grade and were dried by standard methods[17] and distilled under nitrogen prior to their use.

Syntheses. Ligand. 2-(2-Hydroxyethyl)amino-3-oximobutane, H_2L^1. Hdamo (1.01 g, 10 mmol) and Hea (0.61 g, 10 mmol) were

(4) (a) Alexiou, M.; Dendrinou-Samara, C.; Raptopoulou, C. P.; Terzis, A.; Kessissoglou, D. P. *Inorg. Chem.* **2002**, *41*, 4732. (b) Psomas, G.; Stemmler, A. J.; Dendrinou-Samara, C.; Bodwin, J. J.; Schneider, M.; Alexiou, M.; Kampf, J. W.; Kessissoglou, D. P.; Pecoraro, V. L. *Inorg. Chem.* **2001**, *40*, 1562. (c) Psomas, G.; Dendrinou-Samara, C.; Alexion, M.; Tsobos, A.; Raptopoulou, C. P.; Terzis, A.; Kessisoglou, D. P. *Inorg. Chem.* **1998**, *37*, 6556.

(5) For example, see: (a) Liu, S.-X.; Lin, S.; Lin, B.-Z.; Lin, C.-C.; Huang, J.-Q. *Angew. Chem., Int. Ed.* **2001**, *40*, 1084. (b) John., R. P.; Park, M.; Moon, D.; Lee, K.; Hong, S.; Zou, Y.; Hong, C. S.; Lah, M. S. *J. Am. Chem. Soc.* **2007**, *129*, 14142. (c) John, R. P.; Lee, K.; Lah, M. S. *Chem. Commun.* **2004**, 2660. (d) Liu, W.; Lee, K.; Park, M.; John, R. P.; Moon, D.; Zou, Y.; Liu, X.; Ri, H.-C.; Kim, G. H.; Lah, M. S. *Inorg. Chem.* **2008**, *47*, 8807. (e) Moon, D.; Lee, K.; John, R. P.; Kim, G. H.; Suh, B. J.; Lah, M. S. *Inorg. Chem.* **2006**, *45*, 7991. (f) Piotrowski, H.; Polborn, K.; Hilt, G.; Severin, K. *J. Am. Chem. Soc.* **2001**, *123*, 2699. (g) Saalfrank, R. W.; Trummer, S.; Reimann, U.; Chowdhry, M. M.; Hampel, F.; Waldmann, O. *Angew. Chem., Int. Ed.* **2000**, *39*, 3492. (h) Xu, Z.; Thompson, L. K.; Milway, V. A.; Zhao, L.; Kelly, T.; Miller, D. O. *Inorg. Chem.* **2003**, *42*, 2950. (i) Yamanari, K.; Ito, R.; Yamamoto, S.; Konno, T.; Fuyuhiro, A.; Fujioka, K.; Arakawa, R. *Inorg. Chem.* **2002**, *41*, 6824.

(6) (a) Saalfrank, R. W.; Bernt, I.; Hampel, F. *Angew. Chem., Int. Ed.* **2001**, *40*, 1700. (b) Saalfrank, R. W.; Bernt, I.; Hampel, F. *Chem.—Eur. J.* **2001**, *7*, 2770. (c) Saalfrank, R. W.; Deutscher, C.; Sperner, S.; Nakajima, T.; Ako, A. M.; Uller, E.; Hampel, F.; Heinemann, F. W. *Inorg. Chem.* **2004**, *43*, 4372.

(7) Prakash, M. J.; Lah, M. S. *Chem. Commun.* **2009**, 3326 and references cited therein.

(8) (a) Oshio, H.; Hoshino, N.; Ito, T.; Nakano, M.; Renz, F.; Gütlich, P. *Angew. Chem., Int. Ed.* **2003**, *42*, 223. (b) Sydora, O. L.; Wolczanski, P. T.; Lobkovsky, E. B. *Angew. Chem., Int. Ed.* **2003**, *42*, 2685. (c) Benelli, C.; Parsons, S.; Solan, G. A.; Winpenny, R. E. P. *Angew. Chem., Int. Ed. Engl.* **1996**, *35*, 1825. (d) Watton, S. P.; Fuhrmann, P.; Pence, L. E.; Caneschi, A.; Cornia, A.; Abbati, G. L.; Lippard, J. S. *Angew. Chem., Int. Ed. Engl.* **1997**, *36*, 2774.

(9) (a) Chen, H.; Ogo, S.; Fish, R. H. *J. Am. Chem. Soc.* **1996**, *118*, 4993. (b) Fish, R. H.; Jaouen, G. *Organometallics* **2003**, *22*, 2166 and references cited therein.

(10) (a) Lehaire, M.-L.; Scopelliti, R.; Piotrowski, H.; Severin, K. *Angew. Chem., Int. Ed.* **2002**, *41*, 1419. (b) Grote, Z.; Scopelliti, R.; Severin, K. *J. Am. Chem. Soc.* **2004**, *126*, 16959.

(11) (a) Dendrinou-Samara, C.; Alexiou, M.; Zaleski, C. M.; Kampf, J. W.; Kirk, M. L.; Kessissoglou, D. P.; Pecoraro, V. L. *Angew. Chem., Int. Ed.* **2003**, *42*, 3763. (b) Zaleski, C. M.; Depperman, E. C.; Kampf, J. W.; Kirk, M. L.; Pecoraro, V. L. *Angew. Chem., Int. Ed.* **2004**, *43*, 3912. (c) Zaleski, C. M.; Depperman, E. C.; Dendrinou-Samara, C.; Alexiou, M.; Kampf, J. W.; Kessissoglou, D. P.; Kirk, M. L.; Pecoraro, V. L. *J. Am. Chem. Soc.* **2005**, *127*, 12862.

(12) (a) Fujita, M.; Kwon, Y. J.; Washizu, S.; Ogura, K. *J. Am. Chem. Soc.* **1994**, *116*, 1151. (b) Di Nicola, C.; Karabach, Y. Y.; Kirillov, A. M.; Monari, M.; Pandolfo, L.; Pettinari, C.; Pombeiro, A. J. L. *Inorg. Chem.* **2007**, *46*, 221.

(13) (a) Mandal, D.; Chatterjee, P. B.; Ganguly, R.; Tiekink, E. R. T.; Clérac, R.; Chaudhury, M. *Inorg. Chem.* **2008**, *47*, 584. (b) Mukhopadhyay, S.; Mandal, D.; Ghosh, D.; Goldberg, I.; Chaudhury, M. *Inorg. Chem.* **2003**, *42*, 8439. (c) Ghosh, D.; Mukhopadhyay, S.; Samanta, S.; Choi, K.-Y.; Endo, A.; Chaudhury, M. *Inorg. Chem.* **2003**, *42*, 7189. (d) Bhattacharyya, S.; Weakley, T. J. R.; Chaudhury, M. *Inorg. Chem.* **1999**, *38*, 633. (e) Bhattacharyya, S.; Weakley, T. J. R.; Chaudhury, M. *Inorg. Chem.* **1999**, *38*, 5453. (f) Bhattacharyya, S.; Ghosh, D.; Endo, A.; Shimizu, K.; Weakley, T. J. R.; Chaudhury, M. *J. Chem. Soc., Dalton Trans.* **1999**, 3859.

(14) Audhya, A.; Bhattacharya, K.; Maity, M.; Chaudhury, M. *Inorg. Chem.* **2010**, *49*, 5009.

(15) Angaridis, P. A.; Baran, P.; Boča, R.; Cervantes-Lee, F.; Haase, W.; Mezei, G.; Raptis, R. G.; Werner, R. *Inorg. Chem.* **2002**, *41*, 2219.

(16) (a) Saalfrank, R. W.; Scheurer, A.; Prakash, R.; Heinemann, F. W.; Nakajima, T.; Hampel, F.; Leppin, R.; Pilawa, B.; Rupp, H.; Müller, P. *Inorg. Chem.* **2007**, *46*, 1586. (b) Brechin, E. K.; Soler, M.; Davidson, J.; Parsons, S.; Christou, G. *Chem. Commun.* **2002**, 2252. (c) Saalfrank, R. W.; Nakajima, T.; Mooren, N.; Scheurer, A.; Maid, H.; Hampel, F.; Triefinger, C.; Daub, J. *Eur. J. Inorg. Chem.* **2005**, 1149. (d) Milios, C. J.; Manoli, M.; Rajaraman, G.; Mishra, A.; Budd, L. E.; White, F.; Parsons, S.; Wernsdorfer, W.; Christou, G.; Brechin, E. K. *Inorg. Chem.* **2006**, *45*, 6782. (e) Brechin, E. K.; Soler, M.; Davidson, J.; Hendrickson, D. N.; Parsons, S.; Christou, G. *Chem. Commun.* **2002**, 2252. (f) Wittick, L. M.; Murray, K. S.; Moubaraki, G.; Batten, S. R.; Spiccia, L.; Berry, K. J. *Dalton Trans.* **2004**, 1003. (g) Stamatatos, T. C.; Abboud, K. A.; Christou, G. *Polyhedron* **2009**, *28*, 1880. (h) Stamatatos, T. C.; Christou, G. *Inorg. Chem.* **2009**, *48*, 3308.

(17) Perrin, D. D.; Armarego, W. L. F.; Perrin, D. R. *Purification of Laboratory Chemicals*, 2nd ed.; Pergamon: Oxford, England, 1980.

dissolved in 15 mL of dry diisopropyl ether, and the solution was refluxed for 30 min. The colorless supernatant liquid was decanted off in hot conditions from the gummy sediment and kept at 0 °C for an overnight period to get a white solid. It was collected by filtration and recrystallized from acetonitrile. Yield: 0.70 g (50%). Mp: 85 °C. Its prolonged exposure to aerobic conditions generates a yellow intractable mass of unknown composition. However, when stored under nitrogen at 0 °C, this compound is indefinitely stable. Anal. Calcd for $C_6H_{12}N_2O_2$: C, 49.98; H, 8.39; N, 19.43. Found: C, 50.22; H, 8.01; N, 19.32. ^{1}H NMR (300 MHz, DMSO-d_6, 298 K, δ/ppm): 3.63 (t, 2H, $-CH_2$, $J = 6.25$ Hz); 3.42 (t, 2H, $-CH_2$, $J = 6.25$ Hz); 1.97 (s, 3H, $-CH_3$); 1.88 (s, 3H, $-CH_3$). FT-IR bands (KBr pellet, cm^{-1}): 3176m, 3072w, 2910w, 2754w, 1625s, 1463m, 1352m, 1137m, 1087s, 1054m, 1018m, 671m. ESI-MS (positive ion mode) in CH_3CN: m/z, 145 $[M + H]^+$.

Complexes. $[(NiHL^1)_3(\mu_3\text{-}O)]ClO_4$ (1). Method a. The Schiff-base ligand H_2L^1 (0.14 g, 1 mmol) and triethylamine (0.10 g, 1 mmol) were mixed together in 30 mL of methanol. To this was added $NiCl_2 \cdot 6H_2O$ (0.24 g, 1 mmol) in solid, and the resulting mixture was refluxed for 30 min to get a deep-red solution. It was cooled to room temperature, and solid $NaClO_4$ was added. The solution was left in the air for an overnight period to get dark-red crystals. Yield: 0.17 g (74%). Some of these rectangular block-shaped crystals are of diffraction-grade and used directly for X-ray diffraction analysis. Anal. Calcd for $C_{18}H_{33}N_6O_{11}Ni_3Cl$: C, 29.95; H, 4.57; N, 11.65. Found: C, 29.64; H, 4.49; N, 11.62. ^{1}H NMR (300 MHz, DMSO-d_6, 298 K, δ/ppm): 4.84 (s, 1H, $-OH$); 3.52 (s, 2H, $-CH_2$); 2.95 (s, 2H, $-CH_2$); 1.89 (s, 3H, $-CH_3$); 1.59 (s, 3H, $-CH_3$). FT-IR bands (KBr pellet, cm^{-1}): 3456mb, 3373mb, 2954w, 1600w, 1521m, 1431w, 1375w, 1344m, 1230m, 1116m, 1054sb, 1016m, 754m, 624m. ESI-MS (positive ion mode) in CH_3CN: m/z 621 $[M - ClO_4]^+$.

Method b. Hdamo (0.10 g, 1 mmol) and Hea (0.061 g, 1 mmol) were mixed together in 30 mL of methanol, and the solution was refluxed for 30 min to get a pale-yellow solution. To this were then added $LiOH \cdot H_2O$ (0.08 g, 2 mmol) and $Ni(ClO_4)_2 \cdot 6H_2O$ (0.37 g, 1 mmol) in solid, and the resulting mixture was refluxed further for an additional 1 h to get a deep-red solution. It was left in the air for slow evaporation. A dark-red crystalline compound was obtained within a few days. Yield: 0.15 g (65%). The identity of the product was confirmed by elemental analysis (C, H, and N) and FT-IR spectroscopic analysis. Anal. Calcd for $C_{18}H_{33}N_6O_{11}Ni_3Cl$: C, 29.95; H, 4.57; N, 11.65. Found: C, 29.93; H, 4.55; N, 11.67.

$(Et_3NH)[Ni_4(damo)_4(Hea)_2(ea)_2](ClO_4)_3$ (2). To a stirred methanolic solution (30 mL) of Hdamo (0.10 g, 1 mmol) and triethylamine (0.20 g, 2 mmol) was added $Ni(ClO_4)_2 \cdot 6H_2O$ (0.37 g, 1 mmol) in solid to get a brown solution. Hea (0.06 g) was then added to this solution and refluxed for 1 h, and a dark-red-brown solution was obtained. The reaction mixture was cooled to room temperature and kept in air for 2−3 days to get a dark-red crystalline solid. Yield: 0.23 g (75%). Some of these crystals are of diffraction-quality and are used directly for X-ray crystal structure analysis. Anal. Calcd for $C_{30}H_{66}N_9O_{24}Ni_4Cl_3$: C, 28.17; H, 5.16; N, 9.86. Found: C, 28.17; H, 5.29; N, 9.87. FT-IR bands (KBr pellet, cm^{-1}): 3458mb, 3336m, 3296m, 2927w, 2879w, 1514m, 1477m, 1380m, 1244m, 1120s, 1099s, 1062m, 979m, 653m, 624m. ESI-MS (positive ion mode) in CH_3CN: m/z 621 $[M - ClO_4]^+$.

$[Ni_4(damo)_4(H_2dea)_2(Hdea)_2](ClO_4)_2 \cdot 2H_2O$ (3). To a stirred methanolic solution (30 mL) of Hdamo (0.10 g, 1 mmol) and triethylamine (0.20 g, 2 mmol) was added $Ni(ClO_4)_2 \cdot 6H_2O$ (0.37 g, 1 mmol) in solid to get a brown solution. To this was then added H_2dea (0.11 g, 1 mmol), and the resulting solution was refluxed for 1 h, during which the color changed to dark red. It was cooled to room temperature and kept in air for a few days to get a dark-red crystalline product. Yield: 0.21 g (66%). Some of these crystals are of diffraction-grade and are used directly for X-ray structure analysis. Anal. Calcd for $C_{32}H_{70}N_8O_{26}Ni_4Cl_2$: C, 29.80; H, 5.43; N, 8.69. Found: C, 29.70; H, 5.55; N, 8.23. FT-IR bands (KBr pellet, cm^{-1}): 3427mb, 3272w, 2925w, 1622m, 1471m, 1380m, 1242m, 1120s, 1093sb, 979m, 655m, 622m. ESI-MS (positive ion mode) in CH_3CN: m/z 1152 $[M - ClO_4 - 2H_2O]^+$.

$[Ni_4(dpko)_4(Hea)_2(ea)_2](ClO_4)_2 \cdot 4H_2O$ (4). To a stirred methanolic solution (30 mL) of Hdpko (0.19 g, 1 mmol) and triethylamine (0.20 g, 2 mmol) was added $Ni(ClO_4)_2 \cdot 6H_2O$ (0.37 g, 1 mmol) in solid to get an orange solution. To this was then added Hea (0.06 g, 1 mmol), and the resulting solution was refluxed for 30 min, during which the color of the solution turned red. It was cooled to room temperature and kept in air for an overnight period to get a dark-red crystalline product. Yield: 0.26 g (68%). Some of these block-shaped crystals are of diffraction-grade and are used directly for X-ray structure analysis. Anal. Calcd for $C_{52}H_{66}N_{16}O_{20}Ni_4Cl_2$: C, 40.49; H, 4.28; N, 14.54. Found: C, 40.23; H, 4.18; N, 14.21. FT-IR bands (KBr pellet, cm^{-1}): 3404mb, 3350mb, 3271mb, 3066w, 2927w, 2869w, 1595s, 1525m, 1461s, 1434m, 1380w, 1267m, 1139sb, 1118sb, 1089sb, 1066mb, 705m, 628m. ESI-MS (positive ion mode) in CH_3CN: m/z 1369 $[M - ClO_4 - 4H_2O]^+$.

$[Ni_4(mpko)_4(Hmea)_2(mea)_2](ClO_4)_2$ (5). To a stirred methanolic solution (35 mL) of Hmpko (0.14 g, 1 mmol) and triethylamine (0.20 g, 2 mmol) was added $NiCl_2 \cdot 6H_2O$ (0.24 g, 1 mmol) in solid to get an orange solution. To this was then added Hmea (0.08 g, 1 mmol), and the resulting solution was fluxed for 30 min, during which the color changed to a darker red. The solution was cooled to room temperature; $NaClO_4 \cdot H_2O$ (0.14 g, 1 mmol) in solid was then added and kept in air for an overnight period to get an orange crystalline product. Yield: 0.20 g (65%). Some of these block-shaped crystals are of diffraction-grade and are used directly for X-ray structure analysis. Anal. Calcd for $C_{40}H_{62}N_{12}O_{16}Ni_4Cl_2$: C, 37.71; H, 4.87; N, 13.19. Found: C, 37.55; H, 4.90; N, 13.30. FT-IR bands (KBr pellet, cm^{-1}): 3419mb, 3280m, 2920m, 2866m, 1598s, 1529m, 1471s, 1373w, 1261w, 1176m, 1099sb, 1043m, 702m, 648m. ESI-MS (positive ion mode) in CH_3CN: m/z 1173 $[M - ClO_4]^+$.

Caution! *Perchlorate salts of metal complexes containing organic ligands are potentially explosive*[18] *and should be handled in small quantity with sufficient care.*

Physical Measurements. IR spectroscopic measurements were made on samples pressed into KBr pellets using a Shimadzu 8400S FT-IR spectrometer, while for UV−vis spectral measurements, a Perkin-Elmer Lambda 950 UV−vis−NIR spectrophotometer was employed. The ESI-MS spectra in the positive-ion mode were measured on a QTOF model YA 263 micromass spectrometer. Elemental analyses (for C, H, and N) were performed at IACS on a Perkin-Elmer model 2400 series II CHNS analyzer.

Magnetic measurements on polycrystalline samples were carried out in the 1.8−300 K temperature range on a Quantum Design MPMS-XL magnetometer. The samples of **3**−**5** (11.43, 13.26, and 14.51 mg, respectively) were packed in polyethylene plastic bags (of about $3 \times 0.5 \times 0.02$ cm^3) before measurements. The raw data were corrected for the sample holder and the orbital diamagnetic contributions calculated from Pascal's constant.[19] The samples have been checked for ferromagnetic impurities, which were found to be systematically absent by measuring the field dependence of magnetization at $T = 100$ K. The alternating-current (ac) susceptibility measurements were carried out with an oscillating ac field of 3 Oe at 125 Hz, but it is worth noting that no out-of-phase ac signal has been detected. Note also that when a temperature-independent paramagnetism parameter was included in the fitting procedures, it was always found to be lower than 4×10^{-8} cm^3/mol (without modification of the g and J parameters) and thus considered as not relevant in the described models.

(18) Wolsey, W. C. *J. Chem. Educ.* **1973**, *50*, A335.
(19) *Theory and Applications of Molecular Paramagnetism*; Boudreaux, E. A., Mulay, L. N., Eds.; John Wiley & Sons: New York, 1976.

Table 1. Summary of the Crystallographic Data for Complexes **1** and **3**−**5**

parameter	**1**	**3**	**4**	**5**
composition	$C_{18}H_{33}N_6O_{11}Ni_3Cl$	$C_{32}H_{70}N_8O_{26}Ni_4Cl_2$	$C_{52}H_{66}N_{16}O_{20}Ni_4Cl_2$	$C_{40}H_{62}N_{12}O_{16}Ni_4Cl_2$
fw	721.08	1288.63	1540.95	1272.76
cryst syst	monoclinic	monoclinic	tetragonal	tetragonal
space group	$P2_1/c$	$P2_1/c$	$I4_1/acd$	$P4_2/nbc$
a, Å	9.5896(19)	21.844(4)	17.5819(2)	17.0437(4)
b, Å	20.871(4)	12.601(2)	17.5819(2)	17.0437(4)
c, Å	13.297(3)	22.061(4)	46.2392(12)	18.9961(9)
α, deg	90.00	90.00	90.00	90.00
β, deg	93.671(3)	119.455(2)	90.00	90.00
γ, deg	90.00	90.00	90.00	90.00
V, Å^3	2655.9(9)	5287.4(15)	14293.6(4)	5518.1(3)
ρ_{calc}, Mg/m^3	1.803	1.592	1.432	1.532
temp, K	298(2)	150(2)	298(2)	298(2)
λ(Mo Kα), Å	0.710 73	0.710 73	0.710 73	0.710 73
Z	4	4	8	4
$F(000)/\mu$, mm^{-1}	1488/2.273	2652/1.592	6368/1.189	2640/1.514
$2\theta_{max}$, deg	42.82	51.13	47.14	46.96
reflns collected/unique	13 332/3024	25 749/9810	43 164/2678	42 252/2046
R_{int}/GOF on F^2	0.0869/0.841	0.0479/1.101	0.0678/1.071	0.0540/0.953
no. of param	361	682	236	181
R1[a](F_o), wR2[b](F_o) (all data)	0.0796, 0.1411	0.0888, 0.1817	0.0665, 0.1496	0.0635, 0.1633
largest diff peak, deepest hole, e/Å^3	0.348, −0.471	1.606, −0.663	0.435, −0.425	0.853, −0.492

[a] $R1 = \sum||F_o| - |F_c||/\sum|F_o|$. [b] $wR2 = [\sum[w(F_o^2 - F_c^2)^2]/\sum w(F_o^2)^2]^{1/2}$.

X-ray Crystallography. Suitable crystals of **1** (red block, 0.16 × 0.10 × 0.08 mm^3), **2** (red rhombic, 0.22 × 0.14 × 0.10 mm^3), **3** (red block, 0.30 × 0.22 × 0.12 mm^3), **4** (red block, 0.24 × 0.14 × 0.08 mm^3), and **5** (orange block, 0.28 × 0.20 × 0.16 mm^3) were collected from the respective reaction pots and mounted on glass fibers. Intensity data for the compounds were measured employing a Bruker SMART APEX II CCD diffractometer equipped with a monochromatized Mo Kα radiation (λ = 0.710 73 Å) source using the $\omega/2\theta$ scan technique at 298(2) K [or 150(2) K for **3**]. No crystal decay was observed during data collection. The intensity data were corrected for empirical absorption. In all cases, absorption corrections based on multiscans using the *SADABS* software[20] were applied.

The structures were solved by direct methods[21] and refined on F^2 by a full-matrix least-squares procedure[21] based on all data minimizing $R = \sum||F_o| - |F_c||/\sum|F_o|$, $wR = [\sum[w(F_o^2 - F_c^2)^2]/\sum(F_o^2)^2]^{1/2}$ and $S = [\sum[w(F_o^2 - F_c^2)^2]/(n-p)]^{1/2}$. *SHELXL-97* was used for both structure solutions and refinements.[22] A summary of the relevant crystallographic data and the final refinement details is given in Table 1. For compound **3**, one of the uncoordinated hydroxyethyl fragments (C31−C32−O16) and an alcoholic O atom O12 are disordered over two positions, along with two perchlorate O atoms (O20 and O25); their coordinates and occupancies were fixed using the FVAR facility provided with the *SHELXL-97* software. All non-H atoms (excluding the disordered atoms mentioned) were refined anisotropically. The H atoms were calculated and isotropically fixed in the final refinement [d(C−H) = 0.95 Å, with the isotropic thermal parameter of U_{iso}(H) = 1.2U_{iso}(C)]. The *SMART* and *SAINT* software packages[23] were used for data collection and reduction, respectively. Crystallographic diagrams were drawn using the *DIAMOND* software package.[24]

Results and Discussion

Synthesis. In our earlier communication,[14] we reported a family of discrete μ_3-O-bridged trinickel(II) complexes, $[(NiL)_3(\mu_3\text{-}O)]ClO_4$, using 2-(alkylamino)-3-oximobutane (HL) as the associated ligand. These complexes with inverse 9-metallacrown-3 topology are reluctant to accept OH^- as a guest anion inside their metallacrown cavity, although many similar complexes involving a μ_3-OH bridge are well documented in the literature.[25,26] In order to achieve that goal, our strategy has been to use a tailor-made Schiff-base ligand 2-(2-hydroxyethyl)amino-3-oximobutane (H_2L^1) with an appended OH group, accessible to bridge formation. In the preparative procedure as outlined in Scheme 1, the isolated Schiff-base ligand (H_2L^1) and a stoichiometric amount of $Ni(ClO_4)_2\cdot 6H_2O$ (1:1 mole ratio) have been refluxed together in methanol in the presence of added triethylamine. The product obtained, **1**, is a trinuclear compound with Ni^{II} centers connected by the oximato O atoms from the ligands and the central μ_3-O bridge, providing a 9-MC-3 type of metallacrown topology.[1] The OH groups of the associated $(HL^1)^-$ ligands, as revealed from X-ray crystal structure analysis (see later), are all occupying the *distal* positions in complex **1** with sufficient constraints, forcing them to stay away from coordination, at least in the solid state. In an alternative procedure, when the free amino alcohol (Hea) and Hdamo are refluxed with $Ni(ClO_4)_2\cdot 6H_2O$ (in a 1:1:1 mole ratio) in methanol under preparative conditions similar to those above, the reaction interestingly follows a completely different path. The product this time is a tetranuclear compound, **2**, in which the OH donors of the

(20) *SADABS*, version 2.03; Bruker AXS Inc.: Madison, WI, 2002.
(21) Sheldrick, G. M. *Acta Crystallogr.* **1990**, *46A*, 467.
(22) Sheldrick, G. M. *SHELXL-97, Program for Crystal Structure Refinements*; University of Göttingen: Göttingen, Germany, 1996.
(23) *SAINT*, version 6.02; Bruker AXS Inc.: Madison, WI, 2002.
(24) *DIAMOND, Visual Crystal Structure Information System*, version 3.1; Crystal Impact: Bonn, Germany, 2004.
(25) Hay, R. W.; Perotti, A.; Oberti, R.; Ungaretti, L. *Transition Met. Chem.* **1993**, *18*, 570.
(26) (a) Ferrer, S.; Lloret, F.; Bertomeu, I.; Alzulet, G.; Borrás, J.; García-Granda, S.; Liu-González, M.; Haasnoot, J. G. *Inorg. Chem.* **2002**, *41*, 5821. (b) Casarin, M.; Corvaja, C.; di Nicola, C.; Falcomer, D.; Franco, L.; Monari, M.; Pandolfo, L.; Pettinari, C.; Piccinelli, F.; Tagliatesta, P. *Inorg. Chem.* **2004**, *43*, 5865. (c) Casarin, M.; Corvaja, C.; Di Nicola, C.; Falcomer, D.; Franco, L.; Monari, M.; Pandolfo, L.; Pettinari, C.; Piccinelli, F. *Inorg. Chem.* **2005**, *44*, 6265. (d) Maurizio Casarin, M.; Cingolani, A.; Di Nicola, C.; Falcomer, D.; Monari, M.; Pandolfo, L.; Pettinari, C. *Cryst. Growth Des.* **2007**, *7*, 676. (e) Contaldi, S.; Di Nicola, C.; Garau, F.; Karabach, Y. Y.; Martins, L. M. D. R. S.; Monari, M.; Pandolfo, L.; Pettinari, C.; Pombeiro, A. L. J. *Dalton Trans.* **2009**, 4928.

Scheme 1. Protocol for the Syntheses of Complexes **1** and **2**

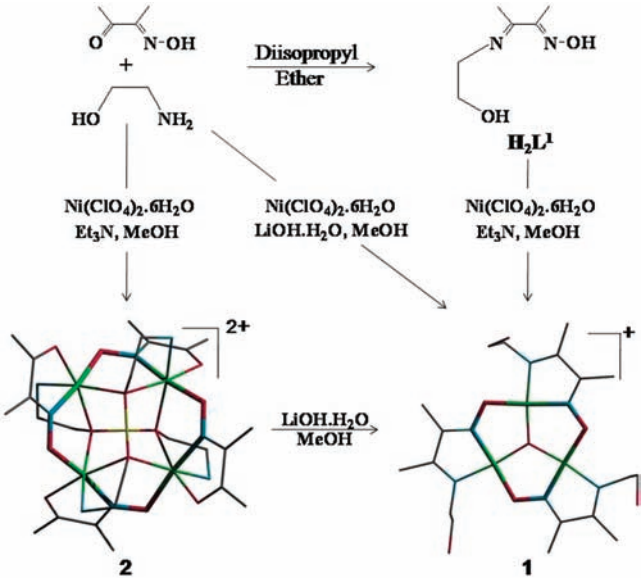

free amino alcohols take up the *proximal* positions to bridge the metal centers, also confirmed by crystal structure analysis. The metal centers in **2** form a new type of inverse metallacrown topology, viz.,12-MC-4, with a larger cavity size that accommodates a pair of hydrogen-bonded $(O-H\cdots O)^-$ anions, contributed by the coordinated amino alcohol ligands attached to the four Ni^{II} centers. Because triethylamine forms a part of the composition of **2**, our strategy next has been to replace Et_3N by LiOH, H_2O just to check whether it has any additional role other than simply a base in the formation of **2**. Surprisingly, in otherwise similar reaction conditions using LiOH as a base, the product obtained is **1**, for which the formation of the Schiff-base ligand (H_2L^1) from its constituents is an obligatory step before the actual complexation can happen. In fact, we have also observed an interesting molecular rearrangement in **2** when it is refluxed with LiOH in methanol to generate **1**, an unprecedented transformation that involves contraction of an inverse metallacrown ring from 12-MC-4 to 9-MC-3 with a concomitant change in the guest anion. Thus, in order to confirm whether avoidance of the Schiff-base formation in the present case is mandatory for generation of a 12-MC-4 metallacrown ring, we subsequently have used a number of combinations of amino alcohol and oxime molecules (Chart 1) where Schiff-base formation is not possible. In all cases without any exception, the products (**3**−**5**) obtained have closely similar 12-MC-4 metallacrown topology with cavities occupied by alkoxo and alcoholic OH donors, connected together by hydrogen bonds.

One important point that deserves to be mentioned here is the selection of nickel salts for the synthesis of **3**−**5**. Unlike in **3** and **4**, the reaction of $Ni(ClO_4)_2\cdot 6H_2O$ with the corresponding oxime, in the case of **5**, generates a yellow insoluble amorphous product that fails to react further with Hmea. The use of $NiCl_2.6H_2O$ as a replacement, followed by the addition of $NaClO_4\cdot H_2O$ in the final step, leads to an efficient synthesis of **5** (see Experimental Section) in ca. 65% yield. Finally, compounds **2**−**5** are soluble appreciably in acetonitrile, while compound **1** is soluble only in *N*,*N*-dimethylformamide (DMF) and dimethyl sulfoxide (DMSO). In solution, these compounds are sufficiently stable.

IR spectra of the complexes (**1**−**5**) show all of the characteristic bands of the coordinated oxime ligands. Prominent among these are two strong signature bands appearing in the regions 1625−1595 and 1180−1115 cm^{-1} due to ν(C=N) and ν(N−O) vibrational modes, respectively.[27,28] In addition, compound **1** displays a broad band at 3176 cm^{-1} due to the ν(O−H) stretching mode for the appended alcohol arm of the Schiff-base ligand. For the remaining compounds (**2**−**5**), however, similar high-energy bands appear in the regions 3460−3420 and 3300−3270 cm^{-1} due to the ν(O−H) and ν(N−H) stretching modes, respectively, of the coordinated amino alcohols. All of these complexes also display a couple of strong- and medium-intensity bands at ca. 1100 and 630 cm^{-1}, respectively, confirming the presence of ionic perchlorate.[29]

Because of the solubility restriction, a ^1H NMR spectrum of **1** has been recorded in DMSO-d_6 at room temperature, as displayed in Figure S1 (see the Supporting Information), showing all of the expected signals of the coordinated Schiff-base ligand, albeit with broad resonance peak shapes. The observed loss of spectral resolution at room temperature motivated us to remeasure the spectra of **1** in DMF-d_7 in the temperature range −15 to +70 °C. The spectral profiles are displayed in Figure S2 in the Supporting Information, which reveal improved resolutions, particularly above room temperature. Thus, at 25 °C, the spectrum includes a pair of singlets of equal intensity appearing at 2.01 and 1.69 ppm due to the C1 and C2 methyl protons, respectively (see the atom-labeling scheme in the inset of Figure S2 in the Supporting Information). While the methylene protons attached to the C3 atom appear in the expected triplet form at 3.05 ppm (J = 4.56 Hz), corresponding protons of the C4 atom, however, show up in the form of a quartet at 3.68 ppm, possibly because of the combined influences of the O5 and C3 protons. The alcoholic proton at O5, which disappears when shaken with D_2O, emerges as a triplet centered at 4.99 ppm (J = 5.74 Hz) because of the vicinal coupling of the C4 protons. Interestingly, all of these features gained enhanced resolution at higher temperatures up to 70 °C and ended up as a broad spectrum when recorded at subambient temperatures. At this stage, it is difficult to be quite sure about the origin of this spectral line broadening at subambient temperatures, but the weak coordination of the free alcoholic OH group to a nearby metal center at low temperatures that would generate paramagnetic five-coordinated Ni^{II} centers might cause such NMR line broadening.

Mass Spectroscopy. ESI-MS data (in the positive ion mode) for complexes **1** and **3**−**5** are listed in the Experimental Section. All of these compounds demonstrate their respective molecular ion peaks due to the $[M - ClO_4]^+$

(27) Mohanty, J. G.; Singh, R. P.; Chakravorty, A. *Inorg. Chem.* **1975**, *14*, 2178.
(28) Papatriantafyllopoulou, C.; Aromi, G.; Tasiopoulos, A. J.; Nastopoulos, V.; Raptopoulou, C. P.; Teat, S. J.; Escuer, A.; Perlepes, S. P. *Eur. J. Inorg. Chem.* **2007**, 2761.
(29) Nakamoto, K. *Infrared and Raman Spectra of Inorganic and Coordination Compounds*, 3rd ed.; Wiley-Interscience: New York, 1978.

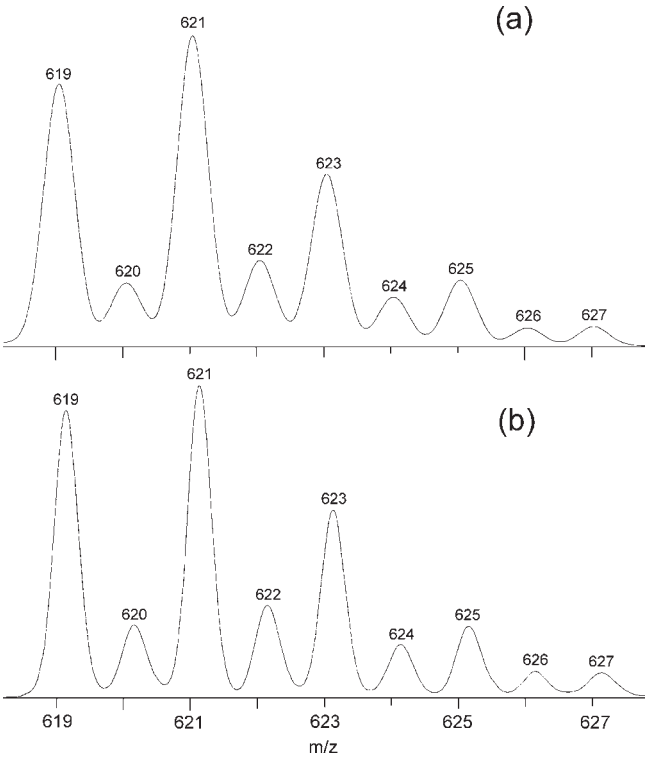

Figure 1. Molecular ion peak in the ESI-MS spectrum (positive ion mode) for complex **1** in acetonitrile with (a) simulated and (b) observed isotopic distributions.

(for **1** and **5**), $[M-ClO_4-2H_2O]^+$ (for **3**), and $[M-ClO_4-4H_2O]^+$ (for **4**) ionic species. Figures 1b and 2b display the isotope distribution patterns for the molecular ion peaks for the two representative compounds **1** and **5**, respectively. Corresponding simulation patterns are displayed in Figures 1a and 2a, respectively. Expected results are also obtained for the remaining compounds, thus providing evidence in favor of the proposed metallacrown topologies for these compounds. Surprisingly, with compound **2**, we were unable to detect the molecular ion peak by ESI-MS done under similar experimental conditions.

Description of Crystal Structures. The molecular structure with the atom-labeling scheme for **1** is displayed in Figure 3, which provides confirmatory evidence in support of its μ_3-O-bridged trinuclear structure that involves appended hydroxyethyl arms, staying away from coordination. Selected metrical parameters of the structure are summarized in Table 2. Complex **1** crystallizes in the monoclinic space group $P2_1/c$ with four molecular weight units accommodated per cell. The cationic species in **1** contains three Ni^{II} centers, one μ_3-O atom, and three tridentate monoanionic ligands $(HL^1)^-$, each bound to a metal center. The individual metal centers are planar, tetracoordinated with N_2O_2 donor sites. The N donors, both imino (N1) and oximino (N2), are contributed by $(HL^1)^-$, while an oximato O atom O1 from an adjacent ligand molecule, together with the central μ_3-O atom O4, completes the remaining donor sites of each of the three equivalent Ni^{II} centers, which are displaced only negligibly by 0.007−0.028 Å from these least-squares mean planes. The C−N and N−O distances of the oxime moieties are in the ranges 1.288(10)−1.302(9) and 1.337(7)−1.346(8) Å, respectively, as expected for the coordinated oximato

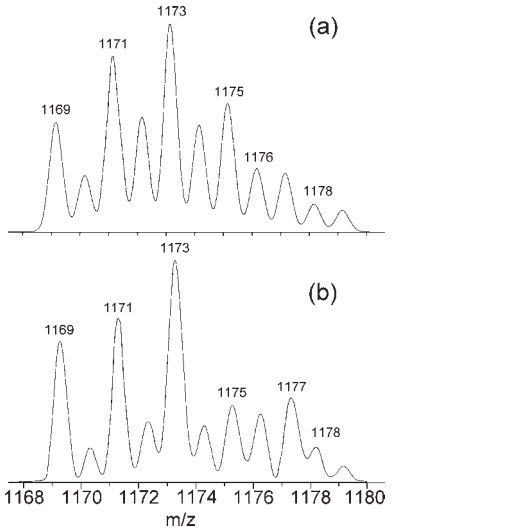

Figure 2. Molecular ion peak in the ESI-MS spectrum (positive ion mode) for complex **5** in acetonitrile with (a) simulated and (b) observed isotopic distributions.

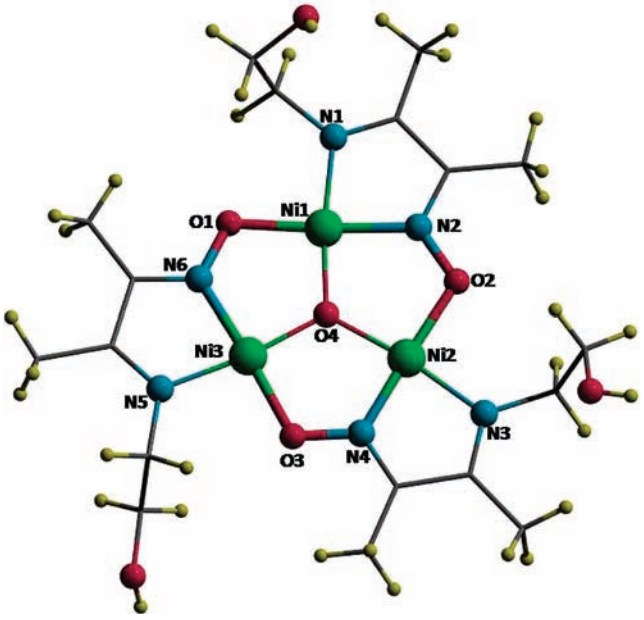

Figure 3. Partially labeled POV-Ray (in ball and stick form) diagram showing the atom-labeling scheme in the cation of **1**. The 9-MC-3 ring topology of the complex is drawn in thick lines.

ligand in deprotonated form.[30] The distances Ni1−O4 1.785(5) Å, Ni2−O4 1.789(5) Å, and Ni3−O4 1.797(5) Å in the central Ni_3O core are almost identical, while the angles Ni1−O4−Ni2 120.4(3)°, Ni2−O4−Ni3 119.9(3)°, and Ni3−O4−Ni1 119.6(3)° are close to 120°. The Ni centers are almost equidistant from each other, Ni1···Ni2 3.102 Å, Ni2···Ni3 3.103 Å, and Ni3···Ni1 3.096 Å, forming an equilateral triangle with the μ_3-O atom O4 displaced marginally by 0.032 Å from the center of this Ni_3 least-squares plane. The bond angles O1−Ni1−N2 176.2(3)°, O2−Ni2−N4 176.3(3)°, and O3−Ni3−N6 176.6(3)° are slightly short of linearity, forcing the metal centers to move marginally toward the central O4 atom, thus generating

(30) Sreerama, S. G.; Pal, S. *Inorg. Chem.* **2002**, *41*, 4843.

Table 2. Selected Bond Distances (Å) and Angles (deg) for **1**

Bond Distances (Å)			
Ni1−O1	1.858(5)	Ni2−N4	1.821(6)
Ni1−N1	1.893(6)	Ni2−O4	1.789(5)
Ni1−N2	1.843(6)	Ni3−O3	1.846(5)
Ni1−O4	1.785(5)	Ni3−N5	1.891(6)
Ni2−O2	1.859(5)	Ni3−N6	1.833(6)
Ni2−N3	1.882(6)	Ni3−O4	1.797(5)
Bond angles (deg)			
O1−Ni1−N1	93.9(3)	O4−Ni2−O2	92.8(2)
N1−Ni1−N2	83.1(3)	O2−Ni2−N4	176.3(3)
N2−Ni1−O4	89.7(3)	O4−Ni2−N3	172.6(3)
O4−Ni1−O1	93.3(2)	O3−Ni3−N5	94.3(3)
O1−Ni1−N2	176.2(3)	N5−Ni3−N6	82.5(3)
O4−Ni1−N1	172.7(3)	N6−Ni3−O4	90.2(3)
O2−Ni2−N3	94.6(3)	O4−Ni3−O3	92.9(2)
N3−Ni2−N4	82.9(3)	O3−Ni3−N6	176.6(3)
N4−Ni2−O4	89.7(3)	O4−Ni3−N5	172.8(3)

precisely an inverse metallacrown topology[1,31] in this case. The appended hydroxyethyl arms are all occupying the *distal* positions with respect to the associated metal centers and prefer not to participate in coordination.

During the continuance of this work, the crystal structure of compound **2** has been reported from another laboratory,[32] which agrees well with our observed data and therefore will not be discussed any further here. Complex **3** also crystallizes in the monoclinic space group $P2_1/c$ with four molecular weight units accommodated in the unit cell. Its perspective view is displayed in Figure 4, which confirms a 12-MC-4 topology with relevant metrical parameters, as summarized in Table 3. The asymmetric unit of this compound comprises one cationic tetranuclear species $[Ni_4(damo)_4(H_2dea)_2(Hdea)_2]^{2+}$, two $(ClO_4)^-$ anions, and two H_2O molecules. All four Ni centers in this molecule are chemically identical, albeit different in crystallographic sense, unlike in **2**, which has a 2-fold axis of symmetry (monoclinic space group $C2/c$).[32] The Ni^{II} centers in this cation are situated at the corners of a square, each having an identical octahedral geometry overall completed by a coordinated iminoxime ($damo^-$) and an amino alcohol ($Hdea^-$) as ligands, both offering N- and O-donor combinations. The remaining two donor sites, comprising oximato and alkoxo O atoms, are coming from an adjacent Ni^{II} unit and play a crucial role in linking the Ni^{II} centers to form a tetrameric structure in which all four metal centers lie on a square plane (Figure 4). The adjacent Ni···Ni separations (Ni1···Ni2 3.408 Å, Ni2···Ni3 3.399 Å, Ni3···Ni4 3.429 Å, and Ni4···Ni1 3.445 Å) are close to each other, while the Ni···Ni···Ni angles are close to 90°, thus generating an arrangement that closely approximates to a square. Each damo ligand chelates a Ni center, for example, Ni1, with the carbonyl O atom O1 and the oximino N atom N1, and connects the adjacent metal center Ni2 through the oximato O linker O2, thus generating the −M−N−O− repeating moiety of the metallacrown topology. Only one of the two alcoholic −OH groups of each H_2dea ligand takes part in metal binding, while the other stays away from coordination. The amino N atom N2 and alcohol O atom O3 bind Ni1 in a chelating mode, while the later, in addition, bridges an adjacent metal center Ni2, which helps to construct the

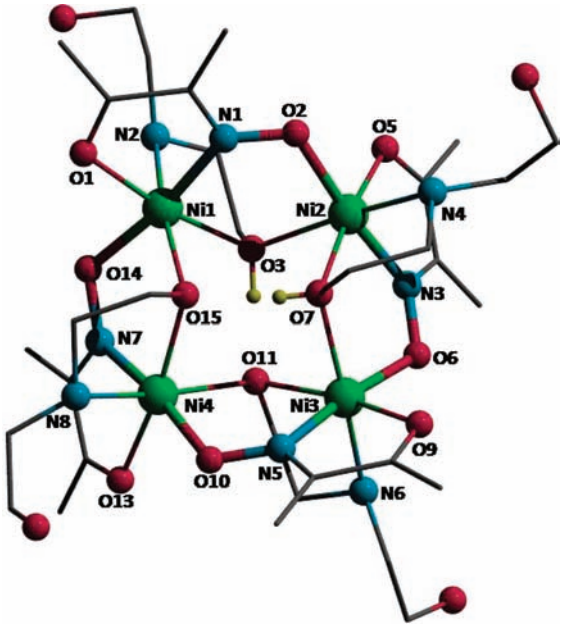

Figure 4. Partially labeled POV-Ray (in ball and stick form) diagram showing the atom-labeling scheme in the cation of **3**. The 12-MC-4 ring topology of the complex is drawn in thick lines.

Table 3. Selected Bond Distances (Å) and Angles (deg) for **3**

Bond Distances (Å)			
Ni1−O14	2.007(3)	Ni3−N5	2.013(4)
Ni1−N1	2.012(4)	Ni3−O6	2.026(3)
Ni1−O3	2.065(3)	Ni3−O9	2.064(4)
Ni1−O1	2.075(3)	Ni3−O11	2.080(3)
Ni1−N2	2.121(4)	Ni3−N6	2.092(4)
Ni1−O15	2.149(3)	Ni3−O7	2.128(3)
Ni2−O2	2.009(3)	Ni4−N7	2.016(4)
Ni2−N3	2.010(4)	Ni4−O10	2.031(4)
Ni2−O5	2.055(4)	Ni4−O13	2.084(4)
Ni2−O7	2.075(4)	Ni4−O15	2.092(3)
Ni2−N4	2.093(5)	Ni4−N8	2.096(5)
Ni2−O3	2.176(3)	Ni4−O11	2.124(3)
Bond Angles (deg)			
O14−Ni1−O1	92.59(14)	O6−Ni3−O9	96.57(15)
O1−Ni1−N2	93.65(15)	O9−Ni3−N6	94.90(17)
N2−Ni1−N1	93.41(18)	N6−Ni3−N5	94.99(18)
N1−Ni1−O3	93.04(14)	N5−Ni3−O11	91.03(15)
O3−Ni1−O15	84.09(12)	O11−Ni3−O7	86.36(13)
O15−Ni1−O14	91.53(13)	O7−Ni3−O6	93.03(13)
O14−Ni1−N1	171.04(15)	O6−Ni3−N5	173.60(16)
O1−Ni1−O3	170.97(14)	O9−Ni3−O11	169.48(14)
N2−Ni1−O15	166.86(14)	N6−Ni3−O7	169.53(16)
O2−Ni2−O5	94.21(14)	O10−Ni4−O13	95.07(15)
O5−Ni2−N4	97.14(18)	O13−Ni4−N8	98.84(18)
N4−Ni2−N3	94.81(18)	N8−Ni4−N7	96.70(2)
N3−Ni2−O7	92.66(15)	N7−Ni4−O15	90.66(15)
O7−Ni2−O3	85.55(13)	O15−Ni4−O11	85.51(12)
O3−Ni2−O2	93.38(13)	O11−Ni4−O10	90.79(13)
O2−Ni2−N3	172.60(15)	O10−Ni4−N7	172.69(16)
O5−Ni2−O7	171.22(14)	O13−Ni4−O15	168.47(14)
N4−Ni2−O3	168.96(16)	N8−Ni4−O11	166.15(19)

(31) (a) Afrati, T.; Dendrinou-Samara, C.; Raptopoulou, C. P.; Terzis, A.; Tangoulis, V.; Kessissoglou, D. P. *Dalton Trans.* **2007**, 5156. (b) Afrati, T.; Dendrinou-Samara, C.; Raptopoulou, C. P.; Terzis, A.; Tangoulis, V.; Tsipis, A.; Kessissoglou, D. P. *Inorg. Chem.* **2008**, *47*, 7545. (c) Halfen, J. A.; Bodwin, J. J.; Pecoraro, V. L. *Inorg. Chem.* **1998**, *37*, 5416.

(32) Mandal, D.; Bertolasi, V.; Aromi, G.; Ray, D. *Dalton Trans.* **2007**, 1989.

metallacrown framework in which the adjacent metal centers are connected by one monatomic (−O−) and one diatomic (−N−O−) bridge, which are lying above and below the square plane through the metal centers. Again, among the four (−N−O−) bridges, two are lying above and two below the Ni_4 plane. Thus, we have a puckered metallacrown ring in this case, as revealed from a lateral view (see below) involving a pair of undulating chains that connect the metal centers of the Ni_4 square. The dihedral angles between the Ni_4 square plane and the bridging planes (involving say, Ni1, N1, O2, Ni2, and O3) that form this fence vary in the range 50.43−53.66°. Interestingly, of the four H_2dea ligands, two are neutral, contributing O3 and O7 bridging atoms, while the remaining two, O11 and O15, are part of the alkoxo groups of the singly deprotonated ligands ($Hdea^-$), as required by the total charge of the complex cationic moiety (2+). Of particular interest are the positions of these alcoholic H atoms, which are located inside the metallacrown cavity. Both H3′ and H7′ protons are separated from their respective alcohol O atoms, viz., O3 and O7, by 0.988 and 0.803 Å, respectively, while their hydrogen-bonded distances from the opposite alkoxo O atoms O11 and O15 are 1.469 and 1.662 Å, respectively. The H7′ and H3′ atoms are located at distances of 1.239 and 1.216 Å, respectively, above and below the Ni_4 quasi-square plane. The trans angles O14−Ni1−N1 171.04(15)°, O2−Ni2−N3 172.60(15)°, O6−Ni3−N5 173.60(16)°, and O10−Ni4−N7 172.69(16)° are all short of linearity, forcing the Ni centers to move toward the center of the cavity, generating an inverse type of metallacrown topology in this case.[1,31]

The crystal structures of the remaining complexes **4** (Figure 5) and **5** (Figure 6) are almost similar and have comparable bond lengths and angles, as summarized in Table 4. Complex **4** crystallizes in a tetragonal space group $I4_1/acd$ ($P4_2/nbc$ for **5**) with eight (four) molecular weight units accommodated per cell. The structure contains a tetranuclear cationic unit $[Ni_4(dpko)_4(Hea)_2(ea)_2]^{2+}$ ($[Ni_4(mpko)_4(Hmea)_2(mea)_2]^{2+}$) counterbalanced by two ClO_4^- anions. The presence of a crystallographic inversion center within this unit implies the equivalence of all four Ni^{II} sites, which are related by a S_4 axis of symmetry. Each Ni^{II} center has a distorted octahedral geometry, completed by a set of N_3O_3 donor combination. As depicted in Figure 5, the basal positions of such a Ni^{II} center in **4** are completed by N3 and O2 donor atoms coming from the chelating amino alcohol (ea), together with the pyridine N atom N1 of the coordinated $dpko^-$ ligand, which also contributes the oximino N-donor atom N2 to occupy one of the axial positions. The remaining axial and equatorial positions of Ni1 are filled up by the oximato O linker O1 and the bridging alkoxide O atom O2′, respectively, both coming from an adjacent Ni center. In this way, two neighboring Ni centers are connected together by a pair of monoatomic (−O−) and diatomic (−O−N−) bridges, generating a 12-MC-4 topology of inverse type (Figure 5), as indicated by the trans angle N2−Ni1−O1 172.75(12)° [173.71(14)°] showing marginal deviation from linearity.[1,31]

Interestingly, unlike compound **3**, the four Ni^{II} centers in **4** and **5** form a perfect square plane with a Ni···Ni separation of 3.453 Å (3.447 Å) and a Ni···Ni···Ni angle of 90° in both cases. As revealed from a lateral view (viewed approximately perpendicularly to the S_4 axis) of

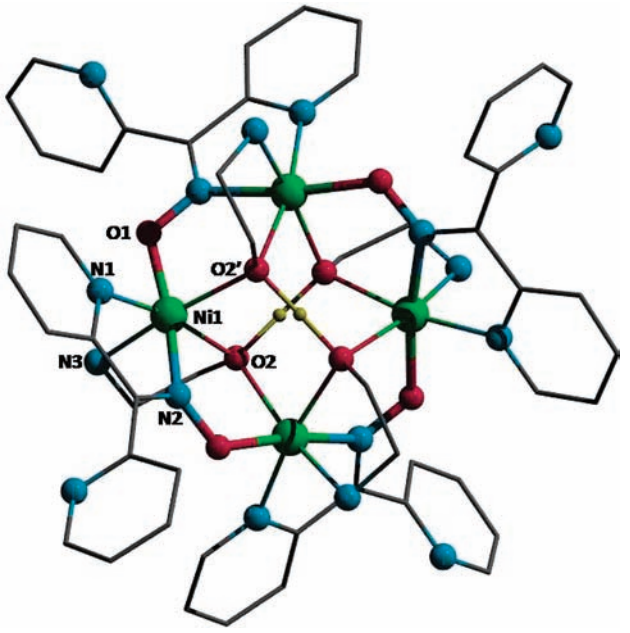

Figure 5. Partially labeled POV-Ray (in ball and stick form) diagram showing the atom-labeling scheme in the cation of **4**. The 12-MC-4 ring topology of the complex is drawn in thick lines.

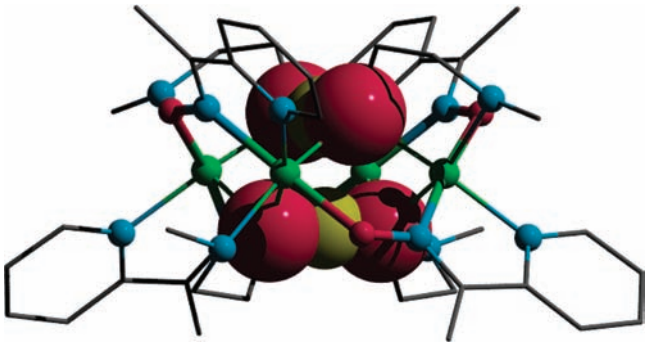

Figure 6. Lateral view (viewed approximately perpendicularly to the S_4 axis) of the POV-Ray diagram of **5** showing the hydrogen-bonded $(-O\cdots H\cdots O-)^-$ guest anions (in a space-fill model) within the inverse 12-MC-4 cavity (thick tubes). Color code: green, Ni; sky blue, N; magenta, O; gray, C; yellow, H.

Table 4. Selected Bond Distances (Å) and Angles (deg) for **4** and **5**

	4	**5**
	Bond Distances (Å)	
Ni1−O1	2.026(3)	2.023(3)
Ni1−N1	2.065(3)	2.054(4)
Ni1−N3	2.079(4)	2.100(4)
Ni1−N2	2.042(3)	2.035(4)
Ni1−O2	2.097(3)	2.104(3)
Ni1−O2′	2.146(3)	2.149(3)
	Bond Angles (deg)	
O1−Ni1−N1	94.35(12)	95.23(15)
N1−Ni1−N3	93.22(17)	93.30(17)
N3−Ni1−N2	93.34(18)	95.33(17)
N2−Ni1−O2	91.23(12)	91.15(14)
O2−Ni1−O2′	84.56(13)	84.32(16)
O2′−Ni1−O1	92.32(10)	92.10(12)
O1−Ni1−N2	172.75(12)	173.71(14)
N1−Ni1−O2	169.23(12)	169.23(14)
N3−Ni1−O2′	167.32(16)	167.02(15)

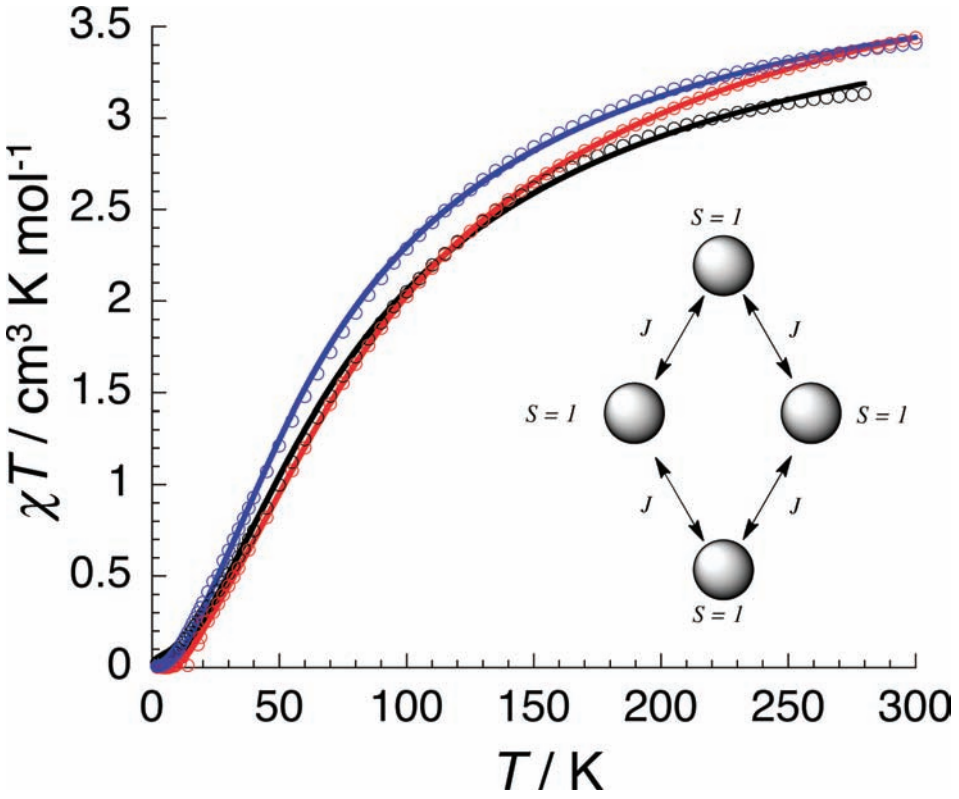

Figure 7. Temperature dependence of the χT products for compounds **3**−**5**. The solid lines [black (**3**), red (**4**), and blue (**5**)] are the best fit obtained with the model described in the text.

the molecular structure of **5** presented in Figure 6, the monoatomic (Ni−O−Ni) and diatomic (Ni−O−N−Ni) bridges are lying on the opposite sides of the metal plane (passing through the green balls) and the bridging pattern is just reversed in the next immediate pair of Ni centers, thus imparting an undulatory mode of propagation of the bridging units along the metallacrown ring. These require two alkoxide O atoms (balls with magenta color) to stay above and two below the metal plane with O−O axes orthogonal to each other, resulting in a distorted tetrahedral arrangement for these O atoms inside the metallacrown cavity. To achieve the total charge balance for the tetranuclear unit (2+), it is required that out of the four alcoholic−OH groups from as many number of Hea (Hmea for **5**) ancillary ligands, two are to be deprotonated. Each of these alkoxide O atoms can be viewed as providing an electron pair projected toward a symmetry-related hydroxo O atom. A H atom (yellow ball) is clearly apparent (from the difference maps) between these two O centers, generating symmetrical hydrogen-bonded units (−O···H···O−) both above and below the metal plane with a very short O···O separation of 2.465 Å (2.437 Å).

Magnetic Properties. Magnetic susceptibility data for the polycrystalline samples of the tetranuclear complexes **3**−**5** have been collected in the 1.8−300 K temperature range in the applied field of 1000 Oe. The corresponding χT vs T plots (χ is the molar magnetic susceptibility per mole of tetranuclear units) are displayed in Figure 7. At room temperature, the χT products are 3.8, 3.8, and 3.3 $cm^3 \cdot K/mol$ for **3**−**5**, respectively, which are slightly lower than the theoretical value of 4.0 $cm^3 \cdot K/mol$ expected for four non-interacting $S = 1$ Ni^{II} ions with $g = 2$ ($C = 1.0$ $cm^3 \cdot K/mol$ each). The result suggests the dominance of antiferromagnetic interactions within these complexes. Upon cooling, the χT product decreases gradually to reach almost zero for all of the compounds, indicating a singlet ground state for these systems. In order to analyze these magnetic behaviors, the magnetic coupling topology (including only the neighboring interactions) deduced from the molecular structures has been considered, as shown in the inset of Figure 7. The simplest tetramer $S = 1$ model with only one coupling parameter J (imposing the S_4 symmetry for **3**, while **4** and **5** display this symmetry axis as shown in the structural part) has been used to fit the magnetic susceptibility data considering the following isotropic spin Hamiltonian (eq 1):

$$\hat{H} = -2J(S_{Ni1}^{|} \cdot S_{Ni2}^{|} + S_{Ni2}^{|} \cdot S_{Ni3}^{|} + S_{Ni3}^{|} \cdot S_{Ni4}^{|} + S_{Ni1}^{|} \cdot S_{Ni4}^{|}) \quad (1)$$

where J is the $Ni^{II}-Ni^{II}$ exchange interaction in the tetranuclear unit (the diagonal interactions between the opposite Ni^{II} atoms of the square unit are considered negligible in this model) and $\boldsymbol{S}_i$ is the spin operator for each Ni^{II} ion, located at the four corners of the square ($S_i = 1$). A theoretical expression (eq 2) of magnetic susceptibility can be derived by applying the van Vleck equation[33] in the weak-field approximation:

$$\chi_0 T = (N g^2 \mu_B{}^2 / k_B)[(2e^{2J/k_BT} + 14e^{6J/k_BT} + 24e^{10J/k_BT} + 50e^{12J/k_BT} + 10e^{14J/k_BT} + 56e^{16J/k_BT} + 60e^{20J/k_BT}) / (1 + 3e^{2J/k_BT} + 11e^{6J/k_BT} + e^{8J/k_BT} + 16e^{10J/k_BT} + 21e^{12J/k_BT} + 5e^{14J/k_BT} + 14e^{16J/k_BT} + 9e^{20J/k_BT})] \quad (2)$$

(33) van Vleck, J. H. *The Theory of Electric and Magnetic Susceptibility*; Oxford University Press: Oxford, U.K., 1932.

As shown in the plots of Figure 7, this model is able to reproduce extremely well the experimental data with J and g equal to −23(1) K and 2.00(8) for **3**, −26.4(4) K and 2.09(3) for **4**, and −20.4(8) K and 2.04(5) for **5**. The sign of J is consistent with moderately strong antiferromagnetic couplings in the tetranuclear units and an $S_T = 0$ spin ground state for these complexes. The observed J values are in the range reported recently for the tetranuclear nickel(II) complexes with similar [Ni_4] topologies.[32,34] As revealed from their crystal structures, two pathways are likely mediating the magnetic interactions: the diatomic O−N oxime link and an alkoxo bridge. Nonplanarity of the former pathway (torsion angles vary in the 12.74−24.54° range) can only generate weak antiferromagnetic coupling between the magnetic orbitals.[35] Therefore, the major contribution to the observed moderately strong antiferromagnetism in **3**−**5** thus comes through the alkoxo pathway, known to be controlled by the Ni−O−Ni bond angle, which is substantially larger (varies in the 106.94−109.33° range) than 90°, thus paving the way for stronger antiferromagnetic interactions in these molecules.[36]

Concluding Remarks

A μ_3-O-bridged inverse metallacrown compound **1** with 9-MC-3 topology has been prepared using a Schiff-base ligand (H_2L^1), generated by the condensation of Hea and Hdamo. Using the same reaction followed by intact Hea and the said oxime, the product is also an inverse metallacrown **2**, but this time with a larger ring size having a 12-MC-4 topology. Interestingly, when **2** is refluxed in methanol with LiOH, it is converted to **1** in almost a quantitative yield, as displayed in Figure 8. This is an example of an unprecedented type of chemical reaction that leads to the contraction of the ring size in an inverse metallacrown topology, as established by X-ray crystallography. Recently, both uranyl- and lanthanide-ion-induced expansion of the regular metallacrown ring from 12-MC-4 to 15-MC-5 topology has been reported in solution, as established through ^{1}H NMR studies.[37] The rearrangement there seems to be necessitated by the accommodation of a larger incoming ion. In the present, however, the replacement of a pair of $(O-H\cdots O)^-$ anions by a smaller $(\mu_3\text{-}O)^{2-}$ anion in the cavity needed contraction of the ring size to accommodate the incoming anion. Thus, formation of a Schiff base is crucial for **1**; this observation is supported by the remaining tetranuclear compounds **3**−**5**, where the chosen combinations of oxime and amino alcohol do not permit Schiff-base formation. Interestingly, all three 12-MC-4 nickel(II) metallacrowns reported thus far have been synthesized using combinations of ligands[4] and can be classified as regular, vacant, and fused types depending on their ring topology.[1] The present series of compounds (**2**−**5**) provides the only example of nickel(II) 12-MC-4 compounds with inverse topology.

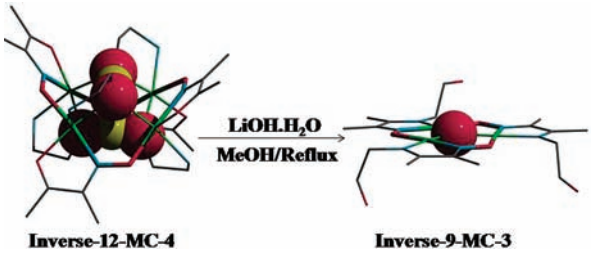

Figure 8. Contraction of the metallacrown cavity size from a 12-membered to a 9-membered ring induced by LiOH through Schiff-base formation of the coordinated ligands.

Acknowledgment. Financial support received from the Council of Scientific and Industrial Research (CSIR), New Delhi, India, is gratefully acknowledged. A.A., M.M., and K.B. also thank the CSIR for the award of Research Fellowships. Crystallographic data were collected at the National Single Crystal X-ray Diffraction Laboratory in the Department of Inorganic Chemistry, Indian Association for the Cultivation of Science. This facility is funded by DST, New Delhi, India. R.C. acknowledges the University of Bordeaux, the CNRS, Région Aquitaine, the GIS Advanced Materials in Aquitaine (COMET Project), and MAGMANet (Grant NMP3-CT-2005-515767) for financial support.

Supporting Information Available: ^{1}H NMR spectra of **1** in DMSO-d_6 and DMF-d_7 (Figures S1 and S2) and X-ray crystallographic files in CIF format for compounds **1** and **3**−**5**. This material is available free of charge via the Internet at http://pubs.acs.org.

(34) (a) Moroz, Y. S.; Kulon, K.; Haukka, M.; Gumienna-Kontecka, E.; Kozlowski, H.; Meyer, F.; Fritsky, I. O. *Inorg. Chem.* **2008**, *47*, 5656. (b) Dawe, L. N.; Thompson, L. K. *Dalton Trans.* **2008**, 3610. (c) Jiang, Y. B.; Kou, H. Z.; Wang, R. J.; Cui, A. L.; Ribas, J. *Inorg. Chem.* **2005**, *44*, 709. (d) Ribas, J.; Monfort, M.; Costa, R.; Solans, X. *Inorg. Chem.* **1993**, *32*, 695. (e) Pavlishchuk, V. V.; Kolotilov, S. V.; Addison, A. W.; Prushan, M. J.; Schollmeyer, D.; Thompson, L. K.; Goreshnik, E. A. *Angew. Chem., Int. Ed.* **2001**, *40*, 4734.

(35) (a) Goodenough, J. B. *Phys. Rev.* **1955**, *100*, 565. (b) Kanamori, J. *J. Phys. Chem. Solids* **1959**, *10*, 87. (c) Hay, P. J.; Thibeault, J. C.; Hoffmann, R. *J. Am. Chem. Soc.* **1975**, *97*, 4884. (d) Kahn, O. *Molecular Magnetism*; VCH Publishers: New York, 1993. (e) Nanda, K. K.; Thompson, L. K.; Bridson, J. N.; Nag, K. *J. Chem. Soc., Chem. Commun.* **1994**, 1337.

(36) Paine, T. K.; Rentschler, E.; Weyhermüller, T.; Chaudhury, P. *Eur. J. Inorg. Chem.* **2003**, 3167.

(37) (a) Parac-Vogt, T. N.; Pacco, A.; Görller-Walrand, C.; Binnemans, K. *J. Inorg. Biochem.* **2005**, *99*, 497. (b) Pacco, A.; Parac-Vogt, T. N.; Van Besien, E.; Pierloot, K.; Görller-Walrand, C.; Binnemans, K. *Eur. J. Inorg. Chem.* **2005**, 3303.